0026-895X/03/6305-993–1001$7.00
MOLECULAR PHARMACOLOGY
Copyright © 2003 The American Society for Pharmacology and Experimental Therapeutics
Mol Pharmacol 63:993–1001, 2003

Vol. 63, No. 5
2258/1060074
Printed in U.S.A.

Spatial Approximation between a Photolabile Residue in Position 13 of Secretin and the Amino Terminus of the Secretin Receptor

MENGWEI ZANG, MAOQING DONG, DELIA I. PINON, XI-QIN DING, ELIZABETH M. HADAC, ZHIJUN LI, TERRY P. LYBRAND, and LAURENCE J. MILLER

Cancer Center and the Department of Molecular Pharmacology and Experimental Therapeutics, Mayo Clinic Scottsdale, Scottsdale, Arizona (M.Z., M.D., D.I.P., X.-Q.D., E.M.H., L.J.M.); and Department of Chemistry and Center for Structural Biology, Vanderbilt University, Nashville, Tennessee (Z.L., T.P.L.)

Received October 31, 2002; accepted February 4, 2002

This article is available online at http://molpharm.aspetjournals.org

ABSTRACT

The amino-terminal domain of class B G protein-coupled receptors is critically important for natural peptide agonist binding and action. The precise role it plays and the molecular basis of the interaction between ligand and this domain are not well understood. In the current work, we have developed a new probe for affinity labeling the secretin receptor through a photolabile benzoyl-phenylalanine residue in position 13. This represented a high affinity ligand (K_i = 56 ± 8 nM) that was a potent full agonist to stimulate cellular cAMP (EC_{50} = 236 ± 22 pM). It covalently labeled the secretin receptor saturably in a single site. This was localized to the amino-terminal domain near the first transmembrane segment using a series of chemical and enzymatic digestions. Edman degradation sequencing of radiolabeled cyanogen bromide and skatole digestion products that were attached to glass beads and further cleaved with endoproteinase Asp-N demonstrated that the labeled residue represented Val^{103}. This is in contrast with previous photoaffinity labeling through positions 6, 18, 22, and 26 of secretin that all labeled the distal end of the amino terminus of this receptor. Together, these five pairs of residue-residue approximations provide important constraints to better understand the molecular conformation of the agonist-bound receptor.

Insights into the molecular basis of agonist ligand binding and activation of a receptor may facilitate the development and refinement of receptor-active drugs. Class B G protein-coupled receptors include several potentially important drug targets. However, our understanding of the molecular basis of binding of the natural ligands for these receptors and for their activation is not well developed. This reflects the structural differences between the class B G protein-coupled receptors and the more extensively studied class A G protein-coupled receptors, which include rhodopsin, with recent solution of its crystal structure (Donnelly, 1997; Tams et al., 1998; Palczewski et al., 2000). It also reflects the size and structural complexity of the natural ligands for the class B receptors. They are all moderately large peptides that have diffuse pharmacophoric domains (Ulrich et al., 1998). The molecular basis of binding to G protein-coupled receptors is best understood for receptors having small, structurally defined ligands (Ji et al., 1998; Palczewski et al., 2000). As natural ligands for other members of this superfamily get larger, binding domains tend to move toward extracellular loop and tail domains that are much less well defined (Ji et al., 1998).

We have been quite interested in the secretin receptor, a prototypic member of the class B family of G protein-coupled receptors (Ishihara et al., 1991). It is present on ductular epithelial cells of the pancreas and biliary tree, where it mediates the secretion of bicarbonate-rich fluid, as well as on pyloric smooth muscle, gastric mucosa, and Brunner's glands (Ulrich et al., 1998). As for other members of this receptor family (Cao et al., 1995; Couvineau et al., 1995; Mannstadt et al., 1998), mutagenesis studies have focused interest on the amino-terminal tail domain of the secretin receptor as being essential for natural peptide agonist binding (Vilardaga et al., 1995; Holtmann et al., 1995, 1996). These include the loss of function by truncation of this domain or by certain missense mutations in this region and the gain of appropriate selectivity by chimeric receptors that incorporate this domain (Vilardaga et al., 1995; Holtmann et al., 1995, 1996). Additionally, a series of photoaffinity labeling studies have estab-

This work was supported by National Institutes of Health grants DK46577 (to L.J.M.) and NS33290 (to T.P.L.) and by the Fiterman Foundation.

ABBREVIATIONS: CNBr, cyanogen bromide; skatole, BNPS-skatole (2-[2′-nitrophenylsulfenyl]-3-methyl-3-bromoindolenine); BS^3, bis(sulfosuccinimidyl)suberate; HA, hemagglutinin; Endo F, endoglycosidase F; CHO, Chinese hamster ovary; KRH, Krebs-Ringers-HEPES; PMSF, phenylmethylsulfonyl fluoride; STI, soybean trypsin inhibitor.

An erratum has been published:
http://molpharm.aspetjournals.org/content/64/1/193.full.pdf

lished spatial approximation between residues within secretin and the amino-terminal tail domain of the secretin receptor (Dong et al., 1999a,b, 2000, 2002).

Indeed, the amino-terminal tail domain represents one of the signature regions of class B G protein-coupled receptors (Ulrich et al., 1998). It is at least 120 residues long in all members of this family and includes six highly conserved cysteine residues and three intradomain disulfide bonds (Vilardaga et al., 1997; Ulrich et al., 1998; Asmann et al., 2000). These bonds seem to be critically important for receptor function; several members of this family have been shown to be sensitive to chemical reduction and thiol modification (Robberecht et al., 1984; Knudsen et al., 1997). It is likely that these bonds provide a stable and consistent structural motif that contributes to the natural ligand binding domain of these receptors. Unfortunately, these bonds have not been directly mapped in the secretin receptor or in a naturally expressed, glycosylated, and functional receptor in this family. Note that there are reports of the structure and disulfide bonding of bacterially expressed, nonglycosylated peptides representing the amino terminus of the parathyroid hormone (Grauschopf et al., 2000) and corticotropin releasing factor (Perrin et al., 2001) receptors. The relationship of these structures to this domain in intact receptors in this family is still unclear.

It is of particular interest that all four reported photoaffinity labeling studies of the secretin receptor have established spatial approximation not only with the amino-terminal domain but also with the same small portion of this domain (Dong et al., 1999a,b, 2000, 2002). These include use of photolabile ligands with sites of covalent attachment in positions 6, 18, 22, and 26 of secretin analogs. Each of these has labeled receptor residues within the first 36 residues of the receptor. Although this raises the interesting possibility that this region makes an important contribution to a ligand-binding motif, there are not yet adequate data to understand its conformation or its relation to the rest of the amino-terminal domain in an intact receptor.

In the current work, we establish another photolabile analog of secretin that maintains high affinity binding and full biological activity. This provides a new probe to determine spatial approximation with still another position within secretin, now representing position 13 near the turn between two helical domains of the solution structure of this hormone (Bodanszky and Bodanszky, 1986; Clore et al., 1988). We use a series of experimental strategies to ultimately define the receptor residue that is covalently labeled by this probe. Although still within the amino-terminal tail domain of the secretin receptor, this residue is in a distinct region of the tail that has not previously been labeled. This should provide an important new constraint to better understand the molecular basis of the binding of secretin to this receptor.

Materials and Methods

Materials. Cyanogen bromide (CNBr) was from Fluka (Buchs, Switzerland). BNPS-Skatole (Skatole), phenylisothiocyanate, bis(sulfosuccinimidyl)suberate (BS^3), and Iodo-beads iodination reagent (*N*-chloro-benzenesulfonamide) were from Pierce Chemical Co. (Rockford, IL). Endoproteinase Asp-N (sequencing grade, from *Pseudomonas fragi* mutant) and the 12CA5 monoclonal antibody against hemagglutinin (HA) were from Roche Molecular Biochemicals (Indianapolis, IN). Protein G-conjugated agarose was from Calbiochem. *N*-(2-Aminoethyl)-3-amino-propyl glass beads were from Sigma (St. Louis, MO). 10% NuPAGE gels and Multimark protein standards were from Novex (San Diego, CA). Endoglycosidase F (Endo F) was prepared in our laboratory, as described previously (Hadac et al., 1996). All other reagents were of analytical grade.

Synthesis of Peptides. Rat secretin-27 and secretin analogs, including (Tyr^{10})rat secretin-27 and (Tyr^{10},Bpa^{13})rat secretin-27 (Bpa^{13} analog or probe), and the human influenza virus HA epitope tag (PYDVPDYA) were synthesized by manual solid-phase techniques as we described previously (Ulrich et al., 1993). All peptides were purified to homogeneity using reversed-phase high-performance liquid chromatography, with identities of products verified by mass spectrometry.

Radioiodination of Probes. (Tyr^{10})rat secretin-27 and (Tyr^{10},Bpa^{13})rat secretin-27 were radioiodinated using brief exposure to the solid-phase mild oxidant, Iodo-beads, as we have described previously (Ulrich et al., 1993). The radioiodinated peptides were purified by high-performance liquid chromatography to yield specific radioactivities of 2000 Ci/mmol (Ulrich et al., 1993).

Cell Culture. The Chinese hamster ovary cell lines stably expressing the wild-type rat secretin receptor, CHO-SecR, and HA epitope-tagged secretin receptor constructs (SecR-HA37 and SecR-HA79) were previously prepared in our laboratory and fully characterized (Ulrich et al., 1993; Dong et al., 1999b). These cell lines and the nontransfected parental CHO-K1 cell line were maintained in culture on tissue culture plasticware in Ham's F-12 medium supplemented with 5% fetal clone II (Hyclone Laboratories, Logan, UT) in a humidified atmosphere with 5% CO_2 at 37°C. Cells were passaged approximately two times per week.

Plasma Membrane Preparation. Enriched plasma membranes were prepared from receptor-bearing cells, as we described previously (Hadac et al., 1996). Membranes were suspended in Krebs-Ringers-HEPES (KRH) medium (25 mM HEPES, pH 7.4, 104 mM NaCl, 5 mM KCl, 1 mM KH_2PO_4, 2 mM $CaCl_2$, and 1.2 mM $MgSO_4$) containing 1 mM phenylmethylsulfonyl fluoride (PMSF) and 0.01% soybean trypsin inhibitor (STI). Aliquots of membranes were stored at −80°C until ready for use in receptor binding and photoaffinity labeling experiments.

Biological Activity Assay. The agonist activity of (Tyr^{10},Bpa^{13})rat secretin-27 was assessed by measuring cellular cAMP content in response to peptide stimulation (Ganguli et al., 1998; Dong et al., 1999b). Receptor-bearing cells were grown in 24-well plates. Before hormonal stimulation, cells were washed with ice-cold phosphate-buffered saline containing 1.47 mM NaH_2PO_4, 8.2 mM Na_2HPO_4, pH 7.0, and 145 mM NaCl. Cells were stimulated for 30 min at 37°C with increasing concentrations of peptide in 250 μl of KRH medium containing 1 mM 3-isobutyl-1-methylxanthine, 0.01% STI, and 0.2% bovine serum albumin. The reaction was terminated by the addition of 6% perchloric acid, with cell lysates collected and adjusted to pH 5.5 to 6.0 using 30% potassium bicarbonate. Supernatants were vortexed, cleared by centrifugation at 2000*g* for 10 min, and used for quantitation of cAMP using a competition-binding assay (Diagnostic Products Corp, Los Angeles, CA), as described previously (Ganguli et al., 1998). Assays were performed in duplicate and repeated in at least three independent experiments.

Receptor Binding Assay. Binding of (Tyr^{10},Bpa^{13})rat secretin-27 to membranes from secretin receptor-bearing cells was performed as described previously (Hadac et al., 1998; Dong et al., 1999b). In brief, membranes (10 μg of protein) were incubated for 1 h at room temperature with a constant amount (approximately 20,000 cpm) of ^{125}I-(Tyr^{10})rat secretin-27 and increasing concentrations (0–1 μM) of the competing nonradiolabeled secretin analogs in KRH medium containing 0.2% bovine serum albumin, 1 mM PMSF, and 0.01% STI (final volume of 500 μl). A Skatron cell harvester (Sterling, VA) with glass fiber filters that had been pretreated in 0.3% polybrene was used to separate free from bound radioligand. Analysis of binding data were performed using the LIGAND program, and was plotted using routines in the Prism software package

(GraphPad Software, San Diego, CA). Data are reported as the means ± S.E.M. of duplicate determinations from a minimum of three independent experiments.

Photoaffinity Labeling of the Secretin Receptor. Photoaffinity labeling experiments were conducted as we described previously (Dong et al., 1999b). Briefly, enriched plasma membranes (50–100 μg) were incubated for 1 h in the dark at room temperature with ^{125}I-(Tyr^{10},Bpa^{13})rat secretin-27 (50–100 pM) in KRH buffer in the absence and presence of increasing amounts of competing secretin. The reaction mixture was photolyzed for 30 min at 4°C in a Rayonet photochemical reactor (Southern New England Ultraviolet Company, Hamden, CT) equipped with 3500-Å lamps. Membranes were washed twice with KRH buffer and solubilized in SDS sample buffer. Component proteins were separated on 10% SDS-polyacrylamide gels under reducing conditions, and bands of interest were visualized by exposure to Kodak X-ray film at −80°C.

Chemical and Enzymatic Cleavage Of The Secretin Receptor. Deglycosylation of the gel-purified secretin receptor and its relevant fragments was achieved by treatment with Endo F, using techniques described previously (Hadac et al., 1996). The gel-purified native or deglycosylated secretin receptor was subjected to chemical and/or enzymatic cleavage. CNBr cleavage was carried out in 70% formic acid in a 200-μl reaction volume. The mixture was flushed with nitrogen and incubated in the dark at room temperature for 72 h on a rotating platform (Dong et al., 1999a). The chemical cleavage with skatole (2 mg/ml) was performed in 70% acetic acid in a final volume of 200 μl in the dark at 37°C for 48 h (Bisello et al., 1998).

For endoproteinase Asp-N cleavage, receptor samples were reduced and alkylated (Dong et al., 1999b) to prevent aberrant cleavage of cysteine residues. Cleavage was then performed by incubating the sample with 0.2 μg of endoproteinase Asp-N in 25 μl of digestion buffer containing 50 mM sodium phosphate, pH 8.0, and 0.01% SDS at 37°C for 24 h. Products of chemical or/and enzymatic cleavage were analyzed and purified by electrophoresis on 10% NuPAGE gels with MES running buffer. For autoradiography, gels were then dried and exposed to X-ray film with intensifying screens at −80°C. The apparent molecular weights of the radioactive bonds were determined by interpolation on a plot of the mobility of the appropriate Multimark protein standards versus the log values of their apparent masses.

Immunoprecipitation of Photoaffinity-Labeled Secretin Receptor and Its Relevant Fragments. The radioactive bands of interest were excised from gels, eluted, and lyophilized. This material was solubilized in 200 μl of immunoprecipitation buffer containing 50 mM Tris-HCl, pH 7.4, 150 mM NaCl, 1 mM EDTA, 2 mM $MgCl_2$, 1 mM dithiothreitol, 2 mM PMSF, 0.1% SDS, 0.5% Nonidet P-40, and 0.2% bovine serum albumin. Samples were centrifuged at 20,800*g* for 10 min at 4°C to remove insoluble material. The resulting supernatant was divided equally into two tubes, one containing 25 μM competing HA peptide and both having 3 μg of anti-HA monoclonal antibody. After incubation with gentle shaking at room temperature for 2 h, 15 μl of protein G-agarose was added. After incubation for an additional 2 h, the agarose beads were pelleted by centrifugation at 6,000 rpm for 1 min and washed. Antigen bound to the pellet was eluted in SDS sample buffer and resolved by NuPAGE gel electrophoresis.

Radiochemical Sequencing. Radiochemical sequencing was performed to identify the secretin receptor residue that was labeled with the probe. This offered unique problems that required a special approach. For this, the radiolabeled, deglycosylated CNBr fragment of the secretin receptor and its product of skatole digestion were purified on gels and coupled to *N*-(2-aminoethyl)-3-amino-propyl glass beads through their amino groups using BS^3. For this, 10 mg of glass beads was incubated on ice for 30 min in 50 μl of 10 mM BS^3 in reaction buffer containing 20 mM sodium phosphate, pH 7.5, and 0.15 M NaCl. The beads were then washed twice with the same buffer. Receptor fragments in 200 μl of the reaction buffer containing 0.01% SDS were conjugated to the BS^3-derivatized beads overnight at 4°C. The beads were then pelleted by low-speed centrifugation, and unreacted cross-linker was quenched by incubation with 200 μl of 50 mM Tris-HCl, pH 6.8, in the reaction buffer for 10 min.

Beads were then washed with 200 μl of endoproteinase Asp-N digestion buffer, resuspended in 20 μl of buffer containing 5 μl of endoproteinase Asp-N (0.2 μg), and allowed to react overnight at 37°C. The receptor fragments coupled to the glass beads were then washed sequentially with methanol, methanol/water (1:1, v/v), and methanol. Manual Edman degradation sequencing was performed directly on the beads using techniques that we have described previously (Ji et al., 1997). Radioactivity eluted in each cycle was quantified using a γ-spectrometer.

Molecular Modeling. Threading algorithms were used to identify plausible tertiary folds for the amino-terminal domain (the first 124 residues minus the signal peptide sequence) of the secretin receptor. Extensive searches defined a 93-residue fragment from *S*-adenosylmethionine synthetase (Protein Data Bank code: 1MXA) as the most reasonable structural template. A three-dimensional model for the amino-terminal domain was generated using the *S*-adenosylmethionine synthetase template with the program Modeler (Sali and Blundell, 1993). Residues 111 to 124 were modeled as an extended conformation, because the structural template does not provide meaningful guidance for this segment of the receptor amino terminus. The NMR-derived solution structure for secretin (Clore et al., 1988) was used as the starting structure for the peptide-receptor complex models. Initial manual peptide docking to the receptor amino terminal domain was guided by the experimental constraints, followed by molecular mechanical structure refinement. Initial models were first subjected to 100 steps of in vacuo conjugate gradient energy minimization with no constraints, following by molecular dynamics simulation using a generalized Born model. Harmonic constraints were used in early stages of molecular dynamics simulation to maintain the peptide hormone conformation close to the NMR solution structure, and five additional constraints were applied to impose peptide-receptor contacts determined from the photoaffinity-labeling experiments. Molecular dynamics simulations were started at 10 K, and the temperature was increased via a linear gradient to 300 K over a 10-pS interval. Harmonic constraints for photoaffinity label contacts were likewise increased gradually from 5.0 kcal/mol/Å to 40.0 kcal/mol/Å over the course of the molecular dynamics simulations. The last configuration from each simulation was then energy minimized with no harmonic constraints to generate final structures for the complex. The amino-terminal domain of the receptor was then attached to a model of the 7-helix bundle domain for the secretin receptor derived directly from a rhodopsin crystal structure (Palczewski et al., 2000) to generate a clearer picture of the spatial and topological constraints the helix bundle imposes on the receptor extracellular domain.

Threading calculations were performed with THREADER 3.3 (Jones et al., 1992) and 123D+ (Alexandrov et al., 1995). All energy minimization and molecular dynamics calculations were performed using AMBER 7 (Casa et al., 2002). All interactive molecular graphics model building and analysis were performed using PSSHOW (Swanson, 1995).

Results

Characterization of (Tyr^{10},Bpa^{13})Rat Secretin-27. This probe was synthesized, purified to homogeneity, and characterized by mass spectrometry. It was also functionally characterized, to determine its ability to bind to the wild-type secretin receptor and to stimulate intracellular cAMP accumulation in secretin receptor-bearing CHO-SecR cells (Fig. 1). The Bpa^{13} analog bound to its receptor specifically and saturably, with affinity slightly lower than natural secretin (Bpa^{13} analog, K_i = 56 ± 8 nM; secretin, K_i = 12 ± 3 nM).

This secretin analog was fully efficacious but slightly less potent than natural secretin. It stimulated cAMP responses in a concentration-dependent manner with an EC_{50} of 236 ± 22 pM (secretin, EC_{50} = 79 ± 9 pM).

Photoaffinity Labeling of the Secretin Receptor. Plasma membranes from the CHO-SecR cell line were used for affinity labeling with the Bpa^{13} probe (Fig. 2). This analog specifically and saturably labeled a protein migrating at M_r ~70,000 on a 10% SDS-polyacrylamide gel electrophoresis gel. This was completely displaced by unlabeled secretin in a concentration-dependent manner (IC_{50} = 20 ± 5 nM) and was not present in affinity-labeled nonreceptor-bearing CHO cell membranes. As expected, the labeled receptor band shifted to M_r ~42,000 after deglycosylation with Endo F. These bands migrated identically to those labeled with Bpa^6, $(BzBz)Lys^{18}$, Bpa^{22}, and Bpa^{26} analogs of secretin that we reported previously (Dong et al., 1999a,b, 2000, 2002).

Identification of the Domain of Labeling. The domain of covalent labeling of the secretin receptor with the Bpa^{13} probe was identified by sequential chemical and enzymatic cleavage reactions. CNBr cleavage was used to provide the first indication of the domain of labeling with the Bpa^{13} probe, as it did previously for the labeling of secretin receptor domains with Bpa^6, $(BzBz)Lys^{18}$, Bpa^{22}, and Bpa^{26} analogs (Dong et al., 1999a,b, 2000, 2002). Theoretically, CNBr cleavage of the secretin receptor should yield 10 fragments, with three containing sites of glycosylation. As shown in Fig. 3, CNBr cleavage of the receptor construct labeled with the Bpa^{13} probe yielded a single radioactive band migrating at M_r ~31,000 that shifted to M_r 9,000 after deglycosylation. Given the mass of the attached Bpa^{13} probe (3341 Da) and the clear evidence of glycosylation, there are two possible candidate fragments that match these data. Both are within the amino terminus of the receptor, with one representing the most distal fragment at the amino terminus (fragment one) and the other representing the segment close to the first transmembrane domain (fragment three). The electrophoretic migration of the CNBr fragment labeled with the Bpa^{13} probe was different from that of the CNBr fragment previously labeled with probes having photolabile residues in positions 6, 18, 22, and 26 (Dong et al., 1999a,b, 2000, 2002).

Immunoprecipitation. The definitive identification of the domain of labeling with the Bpa^{13} probe was achieved by immunoprecipitation of CNBr fragments of the HA-tagged receptors with anti-HA monoclonal antibody. Two well-characterized HA-tagged secretin receptor mutants, SecR-HA37 and SecR-HA79 (Dong et al., 1999b), were used in this series of experiments. Both receptor constructs were affinity labeled with the Bpa^{13} probe and were well recognized by the monoclonal antibody, as demonstrated by the saturability of their immunoprecipitation with HA peptide (Fig. 4). Shown in Fig. 4 is also an autoradiograph of a NuPAGE gel used to separate the products of CNBr cleavage of both receptor mutants labeled with the Bpa^{13} probe. The CNBr cleavage of the labeled SecR-HA79 receptor yielded a band (M_r 25,000 in the middle of Fig. 4, lane 3) that migrated differently from that labeled with the HA37 receptor (M_r 31,000 in the middle of Fig. 4, lane 1). This difference in migration probably reflects the introduction of the HA tag after Asn^{78} in the HA79 construct that eliminated the consensus site for its glycosylation. After deglycosylation of these bands, the HA79 construct fragment (M_r 10,000 in the middle of Fig. 4, lane 4) migrated slightly above the HA37 construct fragment (M_r 9,000 in the middle of Fig. 4, lane 2) to reflect the impact of the inclusion of the nine-residue epitope tag. Immunoprecipitation of the deglycosylated CNBr fragments of HA37 and HA79 secretin receptor constructs labeled with the Bpa^{13} probe revealed that only the fragment from the HA79-tagged receptor was radioactive (Fig. 4, right, lane 4). This provided definitive evidence for the site of covalent labeling with the Bpa^{13} probe to be within CNBr fragment three.

Identification of the Site of Labeling. To further localize the domain of the secretin receptor that was labeled with the Bpa^{13} probe, the labeled CNBr fragment was further cleaved at tryptophan residues with skatole. Theoretically, this reagent will cleave this fragment of the receptor into two glycosylated fragments having core proteins of 1940 and 3834 Da. In the HA79 receptor construct, the fragment analogous to the 1940-Da fragment from the wild-type receptor has a greater mass (3024 Da), because of inclusion of the epitope tag. The Bpa^{13} probe does not contain a tryptophan residue and is therefore not cleaved by skatole. Figure 5 compares the pattern of skatole cleavage of the labeled CNBr fragments derived from wild-type and HA79 receptor constructs. Skatole cleavage of the M_r 31,000 CNBr fragment of the secretin receptor yielded a band migrating at M_r ~13,000 that shifted to M_r ~7,000 after deglycosylation. Skatole cleavage of the deglycosylated M_r 10,000 CNBr fragment from the HA79 receptor construct yielded a labeled fragment migrating at M_r ~7,000, the same size as that from cleavage of the deglycosylated M_r 9,000 CNBr fragment of the HA37 receptor. If the Bpa^{13} probe had labeled the amino-terminal half of the third CNBr fragment, a difference in migration would have been expected for skatole fragments of the HA79 receptor construct (M_r 6,000) and that from the wild-type receptor (M_r 5,000) because of the inclusion of the HA se-

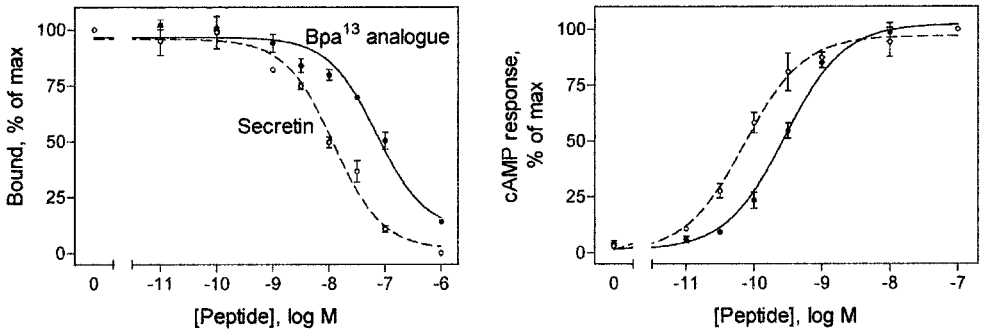

Fig. 1. Binding and biological activity of (Tyr^{10},Bpa^{13})rat secretin-27. Left, the abilities of the Bpa^{13} probe and secretin to compete for binding of ^{125}I-(Tyr^{10})rat secretin-27 to membranes from CHO-SecR cells. Values represent percentages of maximal saturable binding that was observed in the absence of competitor (means ± S.E.M. of data from three independent experiments). Right, the curves representing cAMP accumulation in these cells in response to the Bpa^{13} probe and secretin (means ± S.E.M. of data from three independent experiments, normalized relative to maximal responses).

quence in the former. The similar migration of the skatole fragments from both mutants suggests that the site of labeling with the Bpa[13] probe is within the carboxyl-terminal half of CNBr fragment three.

To further support this identification, immunoprecipitations were performed with the deglycosylated CNBr fragment of the labeled HA79 receptor construct and with its skatole fragment (Fig. 5). As a positive control, the labeled CNBr fragment was well recognized by the anti-HA monoclonal antibody, being precipitated and radioactive (Fig. 5, bottom right, lane 4). However, the immunoprecipitated skatole fragment of the photoaffinity-labeled receptor was not radioactive, suggesting that the region of labeling was not within the amino-terminal half of the third CNBr fragment. This supports the identification of the site of labeling with the Bpa[13] probe as the carboxyl-terminal half of CNBr fragment three, in the region between Ser[91] and Met[123].

To further localize the site of labeling with the Bpa[13] probe, the skatole fragment resulting from cleavage of the CNBr fragment was further cleaved with endoproteinase Asp-N. Theoretically, digestion of this fragment with this enzyme (that cleaves at the amino-terminal side of aspartic acid residues) would yield a glycosylated fragment with peptide core of 3020 Da and a nonglycosylated fragment of 833 Da (Fig. 6). The Bpa[13] probe is also cleaved by endoproteinase Asp-N, yielding a fragment of 1648 Da that contains both the site of covalent attachment through *p*-benzoyl-phenylalanine and the site of radiolabeling. As shown in Fig. 6, the endoproteinase Asp-N cleavage of the skatole-cleaved CNBr fragment (M_r 13,000) yielded a band of M_r ~11,000 that shifted to M_r ~4,500 after deglycosylation. The endoproteinase Asp-N cleavage of the deglycosylated CNBr fragment also yielded a fragment migrating similarly to that of the deglycosylated skatole fragment that had been cleaved with CNBr. This represents the glycosylated fragment between Asp[98] and Met[123] containing the attached truncated probe.

The identification of the specific site of labeling of the secretin receptor with the Bpa[13] probe was achieved by radiochemical sequencing. This was performed with both deglycosylated receptor fragments that had been cleaved with CNBr alone and sequentially with CNBr and skatole, followed by attachment to *N*-(2-aminoethyl)-3-amino-propyl glass beads, where they were further cleaved with endopro-

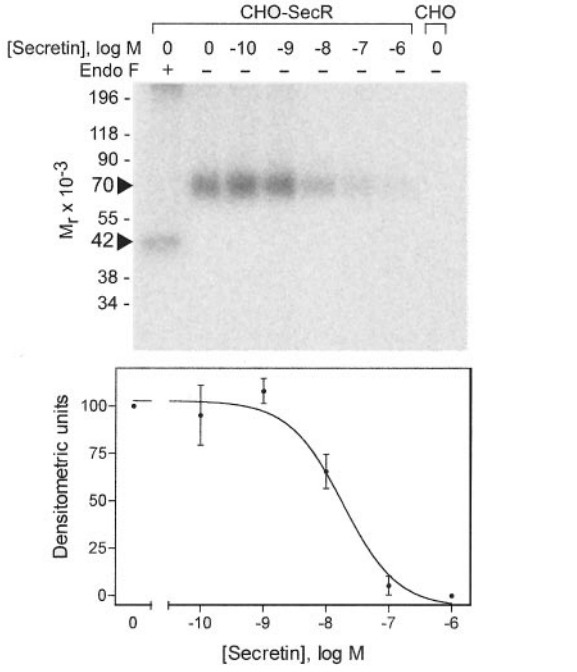

Fig. 2. Photoaffinity labeling of the secretin receptor. Top, a typical autoradiograph of an SDS-polyacrylamide gel electrophoresis gel used to separate products of affinity labeling of secretin receptor-bearing membranes with the Bpa[13] probe in the absence and presence of competing unlabeled secretin. The Bpa[13] probe specifically labeled the M_r 70,000 secretin receptor (core protein M_r 42,000), with this competitively inhibited by secretin. Similar bands were not present in non–receptor-bearing cell membranes treated similarly. Bottom, quantitative densitometry of the labeling of the receptor band in three independent experiments (means ± S.E.M.).

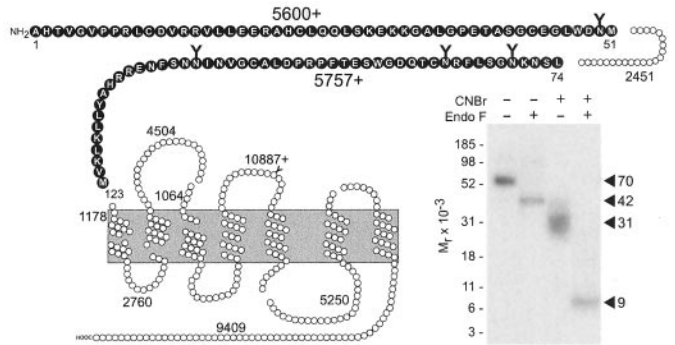

Fig. 3. Cyanogen bromide cleavage of the labeled receptor. Left, a diagram of the predicted sites of CNBr cleavage of the secretin receptor, along with sites of *N*-linked glycosylation. Right, a typical autoradiograph of a 10% NuPAGE gel used to separate the products of CNBr cleavage of the secretin receptor that had been labeled with the Bpa[13] probe. This cleavage yielded a labeled fragment migrating at M_r ~31,000 that shifted to M_r ~9,000 after deglycosylation. Fragments 1 and 3 are the best candidates to represent the domains of labeling with this probe. This pattern is representative of three independent experiments.

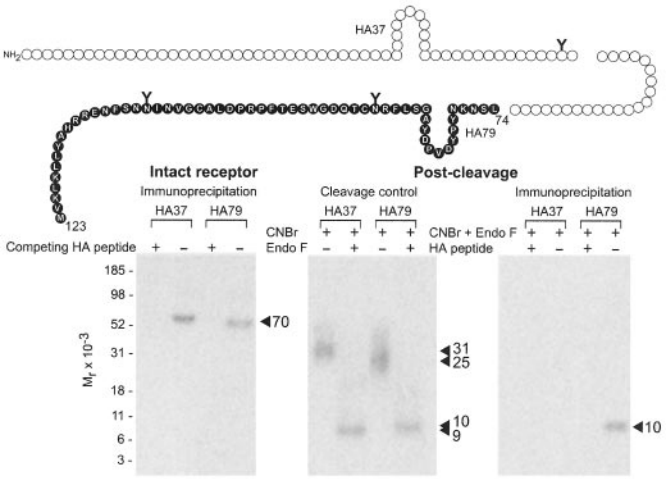

Fig. 4. Immunoprecipitation of epitope-tagged secretin receptor and its CNBr fragment. HA37- and HA79-tagged secretin receptor constructs were labeled with the Bpa[13] probe and were specifically immunoprecipitated by anti-HA monoclonal antibody (left). CNBr cleavage of the affinity-labeled HA37-tagged construct yielded an M_r 31,000 fragment that shifted to M_r 9,000 after deglycosylation, whereas cleavage of the labeled HA79-tagged construct resulted in a band migrating distinctly at M_r ~25,000 that shifted to M_r 10,000 after deglycosylation (middle). Immunoprecipitation of the deglycosylated CNBr fragments revealed that only the immunoprecipitated fragment containing the HA79-tag was radioactive (right). This provides definitive identification of the region of affinity labeling as fragment 3.

teinase Asp-N. After a series of cycles of Edman degradation, the radioactive peak consistently eluted in cycle 6 for both preparations (Fig. 7). As a control, the deglycosylated labeled receptor fragment resulting from CNBr and skatole cleavage that was covalently attached to the beads but not further cleaved with Asp-N was exposed to the same sequencing procedure. No peaks of eluted radioactivity were observed through seven cycles of Edman degradation (data not shown). These studies clearly established that this probe covalently labeled the Val^{103} residue of the secretin receptor.

Molecular Modeling. It was possible to generate a physically plausible three-dimensional model for the amino-terminal domain of the secretin receptor by using a 93 residue fragment from an intact structural domain of *S*-adenosylmethionine synthetase as a template (Fig. 8). Whereas the threading algorithms identified several other proteins with higher Z scores, the matched fragments in these proteins were much shorter peptides that were contained within larger structural domains. The structural model for the secretin receptor amino terminus accommodates the peptide hormone in a conformation quite similar to that observed by NMR for this peptide while free in solution. This model also satisfies all five spatial constraints derived from existing photoaffinity labeling experiments, enables formation of analogous disulfide bonds that have been reported for the extracellular domain of other class B G protein-coupled receptors, and is sterically compatible with a complete model of the secretin receptor based loosely on the helical bundle pattern in the rhodopsin crystal structure. It should be noted, however, that the helix bundle topology and conformations for class B family of G protein-coupled receptors, such as the secretin receptor, are probably rather different from the class A family (e,g., rhodopsin) (Donnelly, 1997; Horn et al., 1998). Therefore, the helix bundle domain of the receptor model reported here should be regarded as a rough approximation at this stage.

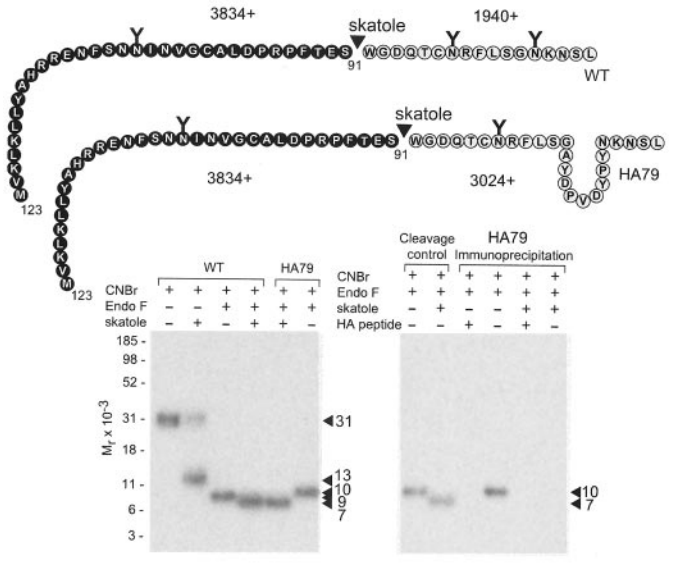

Fig. 5. Skatole cleavage of the labeled CNBr fragments and immunoprecipitation. Top, theoretical skatole cleavage sites of the third CNBr fragment from both wild-type and HA79-tagged secretin receptor constructs. Skatole cleavage of the M_r 31,000 fragment (lane 1) from the wild-type secretin receptor yielded a fragment migrating at M_r 13,000 (lane 2) that shifted to M_r 7,000 (lane 4) after deglycosylation. Of note, the CNBr cleavage of the deglycosylated labeled HA79-tagged receptor yielded a fragment migrating at M_r 10,000 (lane 6), slightly larger than the analogous fragment from the wild-type receptor (lane 3), because of the presence of the inserted HA sequence (bottom left). However, skatole cleavage of both fragments yielded bands with the same apparent molecular mass (M_r 7,000) (lanes 4 and 5), suggesting the absence of HA sequence within the labeled skatole fragment. Thus, the region between Ser^{91} and Met^{123} in the carboxyl-terminal portion of CNBr fragment 3 probably represented the domain of binding the Bpa^{13} probe. Bottom right, results of immunoprecipitation of the CNBr fragment of the HA79-tagged receptor before and after skatole cleavage. Although the immunoprecipitated labeled M_r 10,000 CNBr fragment was radioactive, immunoprecipitation of the labeled M_r 7,000 Skatole fragment did not yield a radioactive band. This further supports the above identification.

Discussion

Photoaffinity labeling of receptor residues using intrinsic probes with photolabile residues incorporated into the pharmacophoric domain of a natural agonist directly provides powerful constraints that can be used to better understand the molecular basis of ligand binding and activation of receptors. In this report, we provide a fifth residue-residue approximation constraint for secretin binding to the secretin receptor. This is particularly noteworthy, because the former four such constraints all involved the covalent labeling of a small subdomain of the amino terminus of the secretin receptor (Dong et al., 1999a,b, 2000, 2002). This was true despite having the sources of these bonds spread throughout the length of secretin, at positions of residues 6, 18, 22, and 26 of this 27-residue linear peptide. These residues are included in paired helical domains in the amino- and carboxyl-terminal halves of secretin (Bodanszky and Bodanszky, 1986) that can be folded to reside adjacent to each other. The position of the photolabile residue in the new probe used in the current report is near the proposed turn between these helices. This position 13 probe also covalently labeled the secretin receptor amino terminus. However, in contrast to the previous stud-

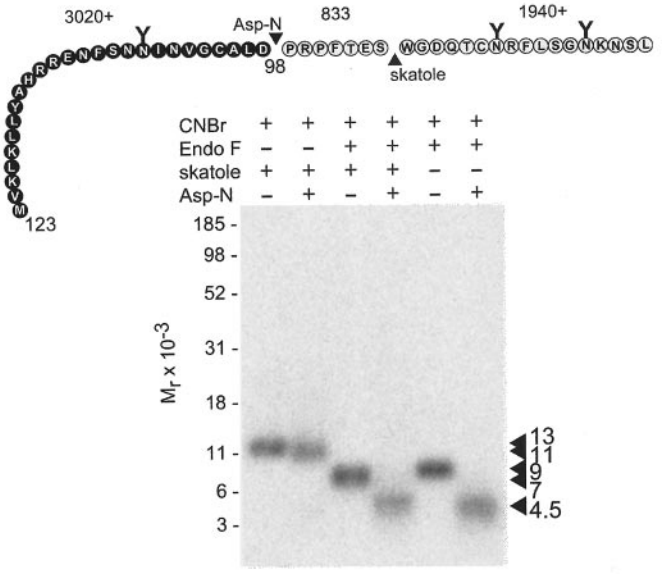

Fig. 6. Further localization of the domain of labeling by endoproteinase Asp-N cleavage. Endoproteinase Asp-N cleavage of the M_r 13,000 fragment (lane 1) resulting from CNBr and skatole cleavage yielded a band migrating at M_r ~11,000 (lane 2). This shifted to M_r ~4,500 (lane 4) after deglycosylaton, the same size (lane 6) as the fragment resulting from Asp-N cleavage of the deglycosylated CNBr fragment from HA79-tagged receptor (lane 5). This suggests that the fragment between Asp^{98} and Met^{123} contains the site of labeling.

ies, this probe labeled a distinct subdomain of the amino terminus.

Identification of the residue labeled by the Bpa[13] probe in the current work was complicated by substantial technical challenges. The domain of labeling was difficult to unambiguously identify, and the determination of the covalently labeled residue within that domain offered other problems. In the experimental strategy used, a number of considerations have to be satisfied. It is critical that the site of covalent attachment of the probe to the receptor and the site of radiolabeling of the probe not be separated from each other in the process of proteolytic cleavage to release the labeled fragment of the receptor or in the process of performing cycles of Edman degradation before arriving at the labeled receptor residue. There is also the requirement that the fragment to be sequenced have the labeled residue near enough its free amino terminus that a reasonable number of cycles of Edman degradation can identify it. The chemistry employed to attach the receptor fragment to a solid-phase support (bead) is also critical. This must be at a point beyond the residues that will be released before arriving at the labeled residue during the performance of cycles of Edman degradation. In addition, the chemistry for covalent capture of the receptor fragment must not at the same time capture the radiolabeled probe. To satisfy all of these conditions, we had to perform extensive and varied cleavage reactions and perform the final cleavage with the receptor fragments already covalently attached to the bead. This resulted in the clear identification of the labeled residue as Val[103], located 22 residues from the predicted position of the first transmembrane segment.

We were previously able to build a limited molecular model of a complex of secretin bound to the first 40 residues of the secretin receptor that could accommodate each of the reported residue-residue approximation constraints that came from all previous photoaffinity labeling studies of this receptor (Dong et al., 1999a,b, 2000, 2002). The receptor residue that was labeled in the current study (Val[103]) is situated between the sixth conserved cysteine residue and the first transmembrane domain, with the previous sites of labeling residing on both sides of the first conserved cysteine residue. This new contact site thus imposed more significant topological constraints on the model structure, and has enabled us to refine an initial working model of the complete amino-terminal domain of the receptor (Fig. 8). The helical bundle domain model reported here is based loosely on the rhodopsin crystal structure. However, as mentioned above, it is thought that class B G protein-coupled receptors probably have rather different helical bundle domain topologies and structures. It will be necessary to obtain additional experimental data to further refine the helix bundle domain of the secretin receptor model.

This series of photoaffinity labeling studies is remarkable for the consistency in labeling a single domain of the secretin receptor, the amino-terminal tail. Indeed, this domain has been identified in truncation and site-directed mutagenesis studies of the secretin receptor (Holtmann et al., 1995, 1996; Vilardaga et al., 1995) and of other class B G protein-coupled receptors (Cao et al., 1995; Couvineau et al., 1995; Mannstadt et al., 1998) to be key for determination of the selectivity of natural ligand binding. Chimeric combinations of receptors in this family have supported the critical role of

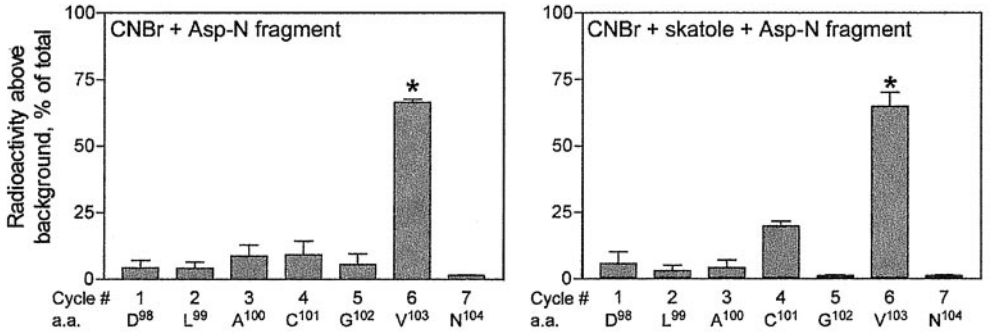

Fig. 7. Identification of the site of labeling by radiochemical sequencing of the labeled fragments. Shown are the radioactive elution profiles from Edman degradation sequencing of the fragments resulting from CNBr and Asp-N cleavage (left) and from CNBr, skatole, and Asp-N cleavage (right) of the deglycosylated secretin receptor labeled with the Bpa[13] probe. For both preparations, the peak in radioactivity consistently appeared in elution cycle 6 in three independent experiments. This represents receptor residue Val[103].

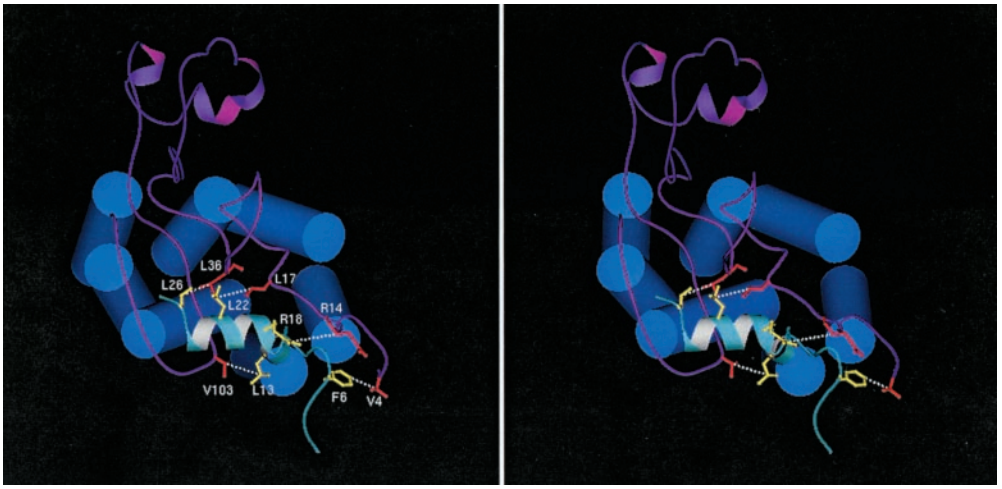

Fig. 8. Model of the secretin peptide/secretin receptor complex. Top view of the secretin peptide hormone bound to the amino-terminal domain of the secretin receptor (stereoscopic pair of images). The receptor amino-terminal domain is shown in purple, with key residues crosslinked in photoaffinity labeling experiments highlighted in red. The peptide hormone is displayed in cyan, with photoaffinity label contact residues shown in yellow. An approximate model of the helix bundle domain proximal to the receptor amino terminus and extracellular loops is shown in blue. The extracellular loops have been removed in this view to facilitate visualization of the peptide contacts with the receptor amino terminus. This image was generated with MOLSCRIPT (Kraulis, 1991).

the receptor amino terminus to determine specificity of binding and activation (Holtmann et al., 1995, 1996; Vilardaga et al., 1995). Clearly, the conserved cysteine residues that probably contribute to the disulfide bonds in this domain are important to constrain its conformation. Such constraints will represent a critical complement to the types of constraints that can come from photoaffinity labeling studies for the elucidation of the molecular basis of ligand binding.

The experimental demonstration clearly indicates that the amino terminus of the secretin receptor is covalently attached to the remainder of the body of this receptor only through its peptide backbone, with no interdomain disulfide bonds (Asmann et al., 2000). This raises two distinct possibilities for the molecular basis of agonist peptide binding to the amino terminus of the receptor, resulting in a conformational change in the cytosolic face of the receptor that facilitates coupling with G proteins. One possibility is that a portion of the secretin peptide interacts directly with the body of this receptor that is distinct from the amino terminus. This would provide a mechanism to exert tension on the receptor body that could lead to a change in conformation. The second possibility is that such tension is provided more indirectly through receptor-receptor interactions that might exist at the base of the amino-terminal domain. A conformational change in the receptor amino terminus could thereby be transmitted to the receptor body, as has been proposed for glucagons and glucagon-like peptide 1 receptor binding (Hjorth and Schwartz, 1996). This could explain why receptor loop domains have been shown to be important in receptor mutagenesis and chimeric receptor studies (Holtmann et al., 1995, 1996). It also explains why there have been inconsistencies in the contribution of the same receptor domain in different chimeric combinations (Holtmann et al., 1995; Vilardaga et al., 2001).

It is notable that affinity labeling studies with photolabile analogs of parathyroid hormone have demonstrated the direct labeling of residues in domains outside of the amino terminus of the parathyroid hormone receptor (Behar et al., 1999; Greenberg et al., 2000). Labeled domains include the first and third extracellular loops and the area high in transmembrane segment six. If this class B G protein-coupled receptor is structurally similar to the secretin receptor, it would suggest that the peptide-binding cleft could reside between the receptor amino-terminal domain and the receptor body. The details of this will need to be further examined in future studies.

Acknowledgments

We acknowledge the help of Dr. Y. Wang, who shared reagents with us for this work, and the excellent technical support of E. Holicky.

References

Alexandrov NN, Nussinov R, and Zimmer RM (1995) Fast protein fold recognition via sequence to structure alignment and contact capacity potentials. *Pacific Symposium on Biocomputing '96: Hawaii, USA, 3–6 January, 1996* (Hunter L, Klein TE eds) pp 53–72, World Scientific Publishing, Singapore.

Asmann YW, Dong M, Ganguli S, Hadac EM, and Miller LJ (2000) Structural insights into the amino-terminus of the secretin receptor: I. Status of cysteine and cystine residues. *Mol Pharmacol* **58:**911–919.

Behar V, Bisello A, Rosenblatt M, and Chorev M (1999) Direct identification of two contact sites for parathyroid hormone (PTH) in the novel PTH-2 receptor using photoaffinity cross-linking. *Endocrinology* **140:**4251–4261.

Bisello A, Adams AE, Mierke DF, Pellegrini M, Rosenblatt M, Suva LJ, and Chorev M (1998) Parathyroid hormone-receptor interactions identified directly by photocross-linking and molecular modeling studies. *J Biol Chem* **273:**22498–22505.

Bodanszky M and Bodanszky A (1986) Conformation of Peptides of the Secretin-VIP-Glucagon Family in Solution. *Peptides* **7**(Suppl 1)**:**43–48.

Cao Y-J, Gimpl G, and Fahrenholz F (1995) The amino-terminal fragment of the adenylate cyclase activating polypeptide (PACAP) receptor functions as a high affinity PACAP binding domain. *Biochem Biophys Res Commun* **212:**673–680.

Case DA, Pearlman DA, Caldwell JW, Cheatham TE III, Wang J, Ross WS, Simmerling CL, Darden TA, Merz KM, Stanton RV, et al. (2002) AMBER 7, Univ. of California, San Francisco.

Clore M, Nilges M, Brunger A, and Gronenborn AM (1988) Determination of the backbone conformation of secretin by restrained molecular dynamics on the basis of interproton distance data. *Eur J Biochem* **171:**479–484.

Couvineau A, Gaudin P, Maoret J-J, Rouyer-Fessard C, Nicole P, and Laburthe M (1995) Highly conserved aspartate 68, tryptophane 73 and glycine 109 in the N-terminal extracellular domain of the human VIP receptor are essential for its ability to bind VIP. *Biochem Biophys Res Commun* **206:**246–252.

Dong M, Asmann YW, Zang MW, Pinon DI, and Miller LJ (2000) Identification of two pairs of spatially approximated residues within the carboxyl terminus of secretin and its receptor. *J Biol Chem* **275:**26032–26039.

Dong M, Wang Y, Hadac EM, Pinon DI, Holicky EL, and Miller LJ (1999a) Identification of an interaction between residue 6 of the natural peptide ligand and a distinct residue within the amino-terminal tail of the secretin receptor. *J Biol Chem* **274:**19161–19167.

Dong M, Wang Y, Pinon DI, Hadac EM, and Miller LJ (1999b) Demonstration of a direct interaction between residue 22 in the carboxyl-terminal half of secretin and the amino-terminal tail of the secretin receptor using photoaffinity labeling. *J Biol Chem* **274:**903–909.

Dong M, Zang MW, Pinon DI, Li Z, Lybrand TP, and Miller LJ (2002) Interaction between four residues distributed through the secretin pharmacophore and a focused region of the secretin receptor amino terminus. *Mol Endocrinol* **16:**2490–2501.

Donnelly D (1997) The arrangement of the transmembrane helices in the secretin receptor family of G-protein-coupled receptors. *FEBS Lett* **409:**431–436.

Ganguli SC, Park CG, Holtmann MH, Hadac EM, Kenakin TP, and Miller LJ (1998) Protean effects of a natural peptide agonist of the G protein-coupled secretin receptor demonstrated by receptor mutagenesis. *J Pharmacol Exp Ther* **286:**593–598.

Grauschopf U, Lilie H, Honold K, Wozny M, Reusch D, Esswein A, Schafer W, Rucknagel KP, and Rudolph R (2000) The N-terminal fragment of human parathyroid hormone receptor 1 constitutes a hormone binding domain and reveals a distinct disulfide pattern. *Biochemistry* **39:**8878–8887.

Greenberg Z, Bisello A, Mierke DF, Rosenblatt M, and Chorev M (2000) Mapping the bimolecular interface of the parathyroid hormone (PTH)-PTH1 receptor complex: spatial proximity between Lys^{27} (of the hormone principal binding domain) and Leu^{261} (of the first extracellular loop) of the human PTH1 receptor. *Biochemistry* **39:**8142–8152.

Hadac EM, Ghanekar DV, Holicky EL, Pinon DI, Dougherty RW, and Miller LJ (1996) Relationship between native and recombinant cholecystokinin receptors—role of differential glycosylation. *Pancreas* **13:**130–139.

Hadac EM, Pinon DI, Ji Z, Holicky EL, Henne R, Lybrand T, and Miller LJ (1998) Direct identification of a second distinct site of contact between cholecystokinin and its receptor. *J Biol Chem* **273:**12988–12993.

Hjorth SA and Schwartz TW (1996) Glucagon and GLP-1 receptors: lessons from chimeric ligands and receptors. *Acta Physiol Scand* **157:**343–345.

Holtmann MH, Ganguli S, Hadac EM, Dolu V, and Miller LJ (1996) Multiple extracellular loop domains contribute critical determinants for agonist binding and activation of the secretin receptor. *J Biol Chem* **271:**14944–14949.

Holtmann MH, Hadac EM, and Miller LJ (1995) Critical contributions of amino-terminal extracellular domains in agonist binding and activation of secretin and vasoactive intestinal polypeptide receptors. Studies of chimeric receptors. *J Biol Chem* **270:**14394–14398.

Horn F, Bywater R, Krause G, Kuipers W, Oliveira L, Paiva ACM, Sander C, and Vriend G (1998) The Interaction of class B G protein-coupled receptors with their hormones. *Recept Channels* **5:**305–314.

Ishihara T, Nakamura S, Kaziro Y, Takahashi T, Takahashi K, and Nagata S (1991) Molecular Cloning and Expression of a CDNA Encoding the Secretin Receptor. *EMBO (Eur Mol Biol Organ) J* **10:**1635–1641.

Ji TH, Grossmann M, and Ji I (1998) G protein-coupled receptors. I. Diversity of receptor-ligand interactions. *J Biol Chem* **273:**17299–17302.

Ji ZS, Hadac EM, Henne RM, Patel SA, Lybrand TP and Miller LJ (1997) Direct identification of a distinct site of interaction between the carboxyl-terminal residue of cholecystokinin and the type A cholecystokinin receptor using photoaffinity labeling. *J Biol Chem* **272:**24393–24401.

Jones DT, Taylor WR, and Thornton JM (1992) A new approach to protein fold recognition. *Nature (Lond)* **358:**86–89.

Knudsen SM, Tams JW, Wulff BS, and Fahrenkrug J (1997) A disulfide bond between conserved cysteines in the extracellular loops of the human VIP receptor is required for binding and activation. *FEBS Lett* **412:**141–143.

Kraulis PJ (1991) MOLSCRIPT: a program to produce both detailed and schematic plots of protein structures. *J Appl Crystallogr* **24:**946–950.

Mannstadt M, Luck MD, Gardella TJ, and Juppner H (1998) Evidence for a ligand interaction site at the amino-terminus of the parathyroid hormone (PTH)/PTH-related protein receptor from cross-linking and mutational studies. *J Biol Chem* **273:**16890–16896.

Palczewski K, Kumasaka T, Hori T, Behnke CA, Motoshima H, Fox BA, Le Trong I, Teller DC, Okada T, Stenkamp RE, et al. (2000) Crystal structure of rhodopsin: A G protein-coupled receptor. *Science (Wash DC)* **289:**739–745.

Perrin MH, Fischer WH, Kunitake KS, Craig AG, Koerber SC, Cervini LA, Rivier JE, Groppe JC, Greenwald J, Moller NS, et al. (2001) Expression, purification and characterization of a soluble form of the first extracellular domain of the human type 1 corticotropin releasing factor receptor. *J Biol Chem* **276:**31528–31534.

Robberecht P, Waelbroeck M, Camus JC, De Neef P, and Christophe J (1984) Importance of disulfide bonds in receptors for vasoactive intestinal peptide and secretin in rat pancreatic plasma membranes. *Biochim Biophys Acta* **773:**271–278.
Sali A and Blundell TL (1993) Comparative protein modeling by satisfaction of spatial constraints. *J Mol Biol* **234:**779–815.
Swanson E (1995) PSSHOW: Silicon Graphics 4D Version, Seattle, Washington.
Tams JW, Knudsen SM, and Fahrenkrug J (1998) Proposed arrangement of the seven transmembrane helices in the secretin receptor family. *Recept Channels* **5:**79–90.
Ulrich CD, Holtmann MH, and Miller LJ (1998) Secretin and vasoactive intestinal peptide receptors: members of a unique family of G protein-coupled receptors. *Gastroenterology* **114:**382–397.
Ulrich CD, Pinon DI, Hadac EM, Holicky EL, Chang-Miller A, Gates LK, and Miller LJ (1993) Intrinsic photoaffinity labeling of native and recombinant rat pancreatic secretin receptors. *Gastroenterology* **105:**1534–1543.
Vilardaga J-P, De Neef P, Di Paolo E, Bollen A, Waelbroeck M, and Robberecht P (1995) Properties of chimeric secretin and VIP receptor proteins indicate the importance of the N-terminal domain for ligand discrimination. *Biochem Biophys Res Commun* **211:**885–891.
Vilardaga JP, Di Paolo E, Bialek C, De Neef P, Waelbroeck M, Bollen A, and Robberecht P (1997) Mutational analysis of extracellular cysteine residues of rat secretin receptor shows that disulfide bridges are essential for receptor function. *Eur J Biochem* **246:**173–180.
Vilardaga JP, Lin I, and Nissenson RA (2001) Analysis of parathyroid hormone (PTH)/secretin receptor chimeras differentiates the role of functional domains in the PTH/PTH-related peptide (PTHrP) receptor on hormone binding and receptor activation. *Mol Endocrinol* **15:**1186–1199.

Address correspondence to: Laurence J. Miller, M.D., Mayo Clinic Scottsdale, S.C. Johnson Research Building, 13400 E. Shea Blvd., Scottsdale, AZ 85259. E-mail: miller@mayo.edu

MOL PHARM

Correction to "Spatial approximation between a photolabile residue in position 13 of secretin and the amino terminus of the secretin receptor"

In the above article [Zang M, Dong M, Pinon DI, Ding X-Q, Hadac EM, Li Z, Lybrand TP, and LJ Miller (2003) *Mol Pharmacol* **63:**993–1001], the accepted date was incorrect. The correct date of acceptance for this article is February 4, 2003.

We regret this error and apologize for any confusion or inconvenience it may have caused.

MOLECULAR PHARMACOLOGY